

## EUROPEAN ORGANIZATION FOR NUCLEAR RESEARCH

CERN/INTC-2002-034

INTC/P-163

September 2002

## Proposal to the INTC Committee

**Neutron Capture Cross Sections of Zr and La:  
Probing Neutron Exposure and Neutron Flux in Red Giant Stars**

**Abstract**

We propose to measure the neutron capture cross sections of  $^{139}\text{La}$ , of  $^{93}\text{Zr}$  ( $t_{1/2}=1.5 \cdot 10^6$  yr), and of all the stable Zr isotopes at n-TOF. The aim of these measurements is to improve the accuracy of existing results by at least a factor of three in order to meet the quality required for using the s-process nucleosynthesis as a diagnostic tool for neutron exposure and neutron flux during the He burning stages of stellar evolution. Combining these results with a wealth of recent information coming from high-resolution stellar spectroscopy and from the detailed analysis of presolar dust grains will shed new light on the chemical history of the universe. The investigated cross sections are also needed for technological applications, in particular since  $^{93}\text{Zr}$  is one of the major long-lived fission products.

*The n-TOF Collaboration*

U. ABBONDANNO<sup>18</sup>, G. AERTS<sup>7</sup>, H. ALVAREZ<sup>28</sup>, S. ANDRIAMONJE<sup>7</sup>,  
 A. ANGELOPOULOS<sup>9</sup>, P. ASSIMAKOPOULOS<sup>12</sup>, C. BACRI<sup>5</sup>, G. BADUREK<sup>1</sup>, P. BAUMANN<sup>6</sup>,  
 F. BEČVÁŘ<sup>37</sup>, H. BEER<sup>8</sup>, J. BENLLIURE<sup>28</sup>, B. BERTHIER<sup>5</sup>, E. BERTHOUMIEUX<sup>7</sup>,  
 F. CALVINO<sup>29</sup>, D. CANO-OTT<sup>24</sup>, R. CAPOTE<sup>27</sup>, P. CARLSON<sup>30</sup>, P. CENNINI<sup>4</sup>, V. CHEPEL<sup>21</sup>,  
 E. CHIAVERI<sup>4</sup>, N. COLONNA<sup>17</sup>, G. CORTES<sup>29</sup>, D. CORTINA<sup>28</sup>, A. COUTURE<sup>34</sup>,  
 S. DABABNEH<sup>8</sup>, M. DAHLFORS<sup>4</sup>, S. DAVID<sup>5</sup>, R. DOLFINI<sup>19</sup>, C. DOMINGO<sup>25</sup>,  
 I. DURAN-ESCRIBANO<sup>28</sup>, C. ELEFThERiADIS<sup>13</sup>, M. EMBID-SEGURA<sup>24</sup>, L. FERRANT<sup>5</sup>,  
 A. FERRARI<sup>4</sup>, L. FERREIRA-LOURENCO<sup>35</sup>, R. FERREIRA-MARQUES<sup>21</sup>,  
 H. FRAIS-KOELBL<sup>3</sup>, W. FURMAN<sup>22</sup>, Y. GIOMATARIS<sup>7</sup>, I. GONCALVES<sup>35</sup>,  
 E. GONZALEZ-ROMERO<sup>24</sup>, A. GOVERDOVSKI<sup>23</sup>, F. GRAMEGNA<sup>16</sup>, E. GRIESMAYER<sup>3</sup>,  
 F. GUNSiNG<sup>7</sup>, R. HAIGHT<sup>32</sup>, M. HEIL<sup>8</sup>, A. HERRERA-MARTINEZ<sup>4</sup>, M. IGASHIRA<sup>39</sup>,  
 K. IOANNIDES<sup>12</sup>, N. JANEVA<sup>36</sup>, E. JERICHA<sup>1</sup>, F. KÄPPELER<sup>8</sup>, Y. KADI<sup>4</sup>,  
 D. KARAMANIS<sup>18</sup>, V. KETLEROV<sup>23</sup>, G. KITIS<sup>13</sup>, P. KOEHLER<sup>33</sup>, V. KONOVALOV<sup>22</sup>,  
 E. KOSSIONIDES<sup>11</sup>, V. LACOSTE<sup>4</sup>, H. LEEB<sup>1</sup>, A. LINDOTE<sup>21</sup>, I. LOPES<sup>21</sup>, M. LOZANO<sup>27</sup>,  
 S. LUKIC<sup>6</sup>, F. MARIE<sup>7</sup>, S. MARKOV<sup>36</sup>, S. MARRONE<sup>17</sup>, J. MARTINEZ-VAL<sup>26</sup>,  
 P. MASTINU<sup>16</sup>, A. MENGONI<sup>4</sup>, P. MILAZZO<sup>18</sup>, E. MINGUEZ<sup>26</sup>, A. MOLINA-COBALLES<sup>27</sup>,  
 C. MOREAU<sup>5</sup>, Y. NAGAI<sup>38</sup>, F. NEVES<sup>21</sup>, H. OBERHUMMER<sup>1</sup>, S. O'BRIEN<sup>34</sup>, T. OHSAKI<sup>39</sup>,  
 J. PANCIN<sup>7</sup>, C. PARADELA<sup>28</sup>, A. PAVLIK<sup>2</sup>, P. PAVLOPOULOS<sup>31</sup>, A. PEREZ-PARRA<sup>24</sup>,  
 J. PERLADO<sup>26</sup>, L. PERROT<sup>7</sup>, V. PESKOV<sup>30</sup>, R. PLAG<sup>8</sup>, A. PLOMPEN<sup>20</sup>, A. PLUKIS<sup>7</sup>,  
 A. POCH<sup>29</sup>, A. POLICARPO<sup>21</sup>, C. PRETEL<sup>29</sup>, J. QUESADA<sup>27</sup>, S. RAMAN<sup>33</sup>, W. RAPP<sup>8</sup>,  
 R. REIFARTH<sup>8</sup>, F. REJMUND<sup>5</sup>, M. ROSETTI<sup>15</sup>, C. RUBBIA<sup>19</sup>, G. RUDOLF<sup>6</sup>,  
 P. RULLHUSEN<sup>20</sup>, J. SALGADO<sup>35</sup>, E. SAVVIDIS<sup>13</sup>, T. SHIMA<sup>38</sup>, J. SOARES<sup>35</sup>, C. STEPHAN<sup>5</sup>,  
 G. TAGLIENTE<sup>17</sup>, K. TAKAHISA<sup>38</sup>, J. TAIN<sup>25</sup>, C. TAPIA<sup>29</sup>, L. TASSAN-GOT<sup>5</sup>, L. TAVORA<sup>35</sup>,  
 M. TERRANI<sup>19</sup>, N. TSANGAS<sup>14</sup>, G. VANNINI<sup>18</sup>, P. VAZ<sup>35</sup>, A. VENTURA<sup>15</sup>,  
 D. VILLAMARIN-FERNANDEZ<sup>24</sup>, M. VINCENTE-VINCENTE<sup>24</sup>, V. VLACHOUDIS<sup>4</sup>,  
 R. VLASTOU<sup>10</sup>, F. VOSS<sup>8</sup>, H. WENDLER<sup>4</sup>, M. WIESCHER<sup>34</sup>, K. WISSHAK<sup>8</sup>, L. ZANINI<sup>4</sup>.

Spokesmen: F. Käppeler, P. Pavlopoulos

- 
- 1) Atominstitut der Österreichischen Universitäten, Technische Universität Wien, Austria
  - 2) Institut für Isotopenforschung und Kernphysik, Universität Wien, Austria
  - 3) Fachhochschule für Wirtschaft und Technik, Wiener Neustadt, Austria
  - 4) CERN, Geneva, Switzerland
  - 5) Centre National de la Recherche Scientifique/IN2P3 - IPN, Orsay, France
  - 6) Centre National de la Recherche Scientifique/IN2P3 - IreS, Strasbourg, France
  - 7) CEA/Saclay - DSM, Gif-sur-Yvette, France
  - 8) Forschungszentrum Karlsruhe GmbH (FZK), Institut für Kernphysik, Germany
  - 9) Astro-Particle Consortium, Nuclear Physics Lab., University of Athens, Greece
  - 10) Astro-Particle Consortium, Nuclear Physics Dep., Technical University of Athens, Greece
  - 11) Astro-Particle Consortium, Nuclear Physics Institute, NCSR "Demokritos", Athens, Greece
  - 12) Astro-Particle Consortium, Nuclear Physics Lab., University of Ioannina, Greece
  - 13) Astro-Particle Consortium, Nuclear Physics Lab., University of Thessaloniki, Greece
  - 14) Astro-Particle Consortium, Nuclear Physics Dep., University of Thrace, Greece
  - 15) ENEA, Bologna, Italy
  - 16) Laboratori Nazionali di Legnaro, Italy
  - 17) Istituto Nazionale di Fisica Nucleare-Bari, Italy
  - 18) Istituto Nazionale di Fisica Nucleare-Trieste, Italy
  - 19) Università degli Studi Pavia, Pavia, Italy
  - 20) CEC-JRC-IRMM, Geel, Belgium
  - 21) Laboratório de Instrumentação e Física Experimental de Partículas - Coimbra & Departamento de Física da Universidade de Coimbra, Portugal
  - 22) Joint Institute for Nuclear Research, Frank Laboratory of Neutron Physics, Dubna, Russia
  - 23) Institute of Physics and Power Engineering, Kaluga region, Obninsk, Russia
  - 24) Centro de Investigaciones Energéticas Medioambientales y Tecnológicas, Madrid, Spain
  - 25) Consejo Superior de Investigaciones Científicas - University of Valencia, Spain
  - 26) Universidad Politécnica de Madrid, Spain
  - 27) Universidad de Sevilla, Spain
  - 28) Universidade de Santiago de Compostela, Spain
  - 29) Universitat Politècnica de Catalunya, Barcelona, Spain
  - 30) Kungliga Tekniska Hogskolan, Physics Department, Stockholm, Sweden
  - 31) Department of Physics and Astronomy - University of Basel, Basel, Switzerland
  - 32) Los Alamos National Laboratory, New Mexico, USA
  - 33) Oak Ridge National Laboratory, Physics Division, Oak Ridge, USA
  - 34) University of Notre Dame, Notre Dame, USA
  - 35) Instituto Tecnológico e Nuclear, Lisbon, Portugal
  - 36) Institute for Nuclear Research and Nuclear Energy, Sofia, Bulgaria
  - 37) Charles University, Prague, Czech Republic
  - 38) Research Center for Nuclear Physics, Osaka University, Osaka, Japan
  - 39) Research Laboratory for Nuclear Reactors, Tokyo Institute of Technology, Tokyo, Japan

# 1 INTRODUCTION

The quest for the origin of the chemical elements in the universe remains a basic motivation for the Nuclear Astrophysics community. For times since the baryonic freeze-out in the Big Bang, stars have been identified as the sites for nucleosynthesis, with some limited, but important contributions from non-stellar processes such as spallation. While most light isotopes are produced via charged particle reactions, the Coulomb barrier becomes prohibitively high above the Fe abundance peak ( $Z \geq 26$ ) for charged particle reactions to play any significant role at energies attainable in a stellar environment. Beyond iron, the only method of production is via neutron induced reactions. There are two dominant neutron capture processes, which differ primarily by the timescale on which they occur. The  $r$  process is a rapid neutron capture process that is related to extremely hot ( $T > 10^9$  K or  $T_8 > 10$  for short), neutron rich ( $n_n \gg 10^{20} \text{ cm}^{-3}$ ) environments. While the  $r$  process will be mentioned briefly later on, the focus of this proposal is on the second neutron capture process, namely the slow neutron capture process ( $s$  process), which operates at significantly lower temperatures and neutron densities ( $T_8 \sim 1 - 3$ ,  $n_n \sim 10^7 - 10^9 \text{ cm}^{-3}$ ).

Approximately half of the abundances in the mass region  $A \gtrsim 56$  can be assigned to each of the two processes. The canonical  $s$  process as proposed originally in 1957 by Burbidge, Burbidge, Fowler and Hoyle [1] takes place in the late He burning stages of stellar evolution. The characteristic feature of the  $s$  process is that neutron captures occur on a time scale of typically 1 yr, much slower than the typical time scale for  $\beta$ -decay. Accordingly, the reaction chain of subsequent neutron captures and  $\beta$ -decays follows the valley of beta stability. This process was first described in a phenomenological way by assuming an exponential distribution of neutron exposures [2, 3]. The abundances produced in the  $s$  process are mostly determined by the neutron capture cross sections of the isotopes involved. These data are required in the energy range from 0.3 to 300 keV corresponding to the respective temperature regime between  $T_8=1$  and 3 ( $T_8$  in units of  $10^8$  K). While this model was useful to understand the global features of the  $s$  process, it fell short in explaining local structures in the solar abundance distribution, but also with respect to the rich variety of  $s$ -abundance patterns observed in AGB stars [4] and in presolar grains [5, 6].

Eventually, realistic stellar models have been developed which can account for the actual stellar conditions under which the  $s$  process is taking place. After first difficulties in reproducing the observed abundances had been overcome, these models were continuously improved to the point where they have now taken precedence as the preferred  $s$ -process models [7]. The success of the stellar  $s$  process models could only be achieved by new developments in neutron capture cross section measurements, which allowed one to reach uncertainties of only a few %. This improved accuracy turned out to be a prerequisite for this application in Nuclear Astrophysics. However, such data are still largely missing, particularly in the mass region  $A \leq 100$  as well as for neutron magic nuclei, where cross sections are small and dominated by single resonances [8].

Accurate  $s$ -process analyses have attracted great interest over the last decade, thanks to progress in astronomical observations and in stellar modelling. In this period, our understanding of the  $s$  process has advanced from the quantitative description of the abundance composition in the solar system towards a comprehensive picture including all aspects of stellar and galactic evolution [9]. This development has emphasized the importance of neutron capture nucleosynthesis for probing the deep interior of Red Giant stars and for following the continuous enrichment of heavy elements during galactic evolution.

The Zr isotopes represent important examples for illustrating these possibilities. The small cross sections of the neutron magic isotopes (such as  $^{90}\text{Zr}$  and  $^{139}\text{La}$ ) act as bottle necks for the reaction flow towards heavier elements. Therefore, these isotopes build up to large abundances and provide evidence for the  $^{13}\text{C}(\alpha, n)$  reaction as the dominant neutron source [7]. Branchings in the reaction path, which occur at unstable isotopes where neutron capture competes with  $\beta$ -decay, have been interpreted as a unique tool for constraining the physical conditions in the He burning zones near the stellar core. A particularly important branching occurs at  $^{95}\text{Zr}$ , which allows one to study the *s*-process neutron flux as outlined below. Lanthanum is important for interpreting the element abundance patterns in very old, metal-poor stars. Since the La abundance is completely represented by  $^{139}\text{La}$ , which is almost of pure *s* origin, it can be used to distinguish the *s*-process component from the products of explosive *r*-process nucleosynthesis. In this way the *s/r*-ratio can be traced over the entire span of galactic chemical evolution, an important aspect for the history of the universe.

Apart from the impact on problems of Nuclear Astrophysics, the  $(n, \gamma)$  cross sections of the stable Zr isotopes are of interest for technological reasons as well. Zirconium constitutes an important component in alloys used as structural material in nuclear reactors, e.g. for cladding of fuel elements. In addition, the unstable isotope  $^{93}\text{Zr}$  ( $t_{1/2} = 1.5 \cdot 10^6$  yr) is one of major long-lived fission products, since it is situated in the maximum of the fission yield distribution.

## 2 THE ASTROPHYSICS CASE

There are essentially three main *s*-process issues related to the proposed measurements on  $^{139}\text{La}$  and on the Zr isotopes. In all these cases, significantly improved cross section information is mandatory for meaningful analyses.

### 2.1 The *s*-Process Branching at $^{95}\text{Zr}$

The zirconium isotopes play a key role for the determination of the neutron density in the He burning zones of Red Giant stars. The principle of this problem is illustrated in Fig. 1, which shows the *s*-process reaction flow in the Zr-Nb-Mo region.

Since  $^{93}\text{Zr}$  is practically stable on the time scale of the *s* process, the neutron capture chain proceeds from  $^{90}\text{Zr}$  to  $^{94}\text{Zr}$  before  $\beta$ -decay comes into play at  $^{95}\text{Zr}$ . Significant *s* production of  $^{96}\text{Zr}$  will, therefore, require that the stellar neutron flux is high enough to compete with  $\beta$ -decay. This question has been studied for the solar abundance distribution [10]. Based on arguments concerning the smooth behavior of the *r*-process component the neutron density was estimated via the classical approach to be  $(4_{-2}^{+3})10^8 \text{ cm}^{-3}$ , in reasonable agreement with the result derived from others branchings [7].

However, when isotopic Zr abundances from the *s*-process enriched envelopes of Red Giants became available via detection of the molecular bands of ZrO [4], it turned out that  $^{96}\text{Zr}$  lines were missing in these spectra. Obviously, the neutron flux in these stars was either weaker than estimated or the stellar  $(n, \gamma)$  rates are smaller than assumed before. A similar but more complex picture emerges from analyses of single, presolar SiC grains, which witness the composition of *s*-processed enriched material from the circumstellar envelopes of Red Giants [6]. The  $^{96}\text{Zr}/^{94}\text{Zr}$  ratios observed in most grains are too small to be satisfactorily explained with present cross section data.

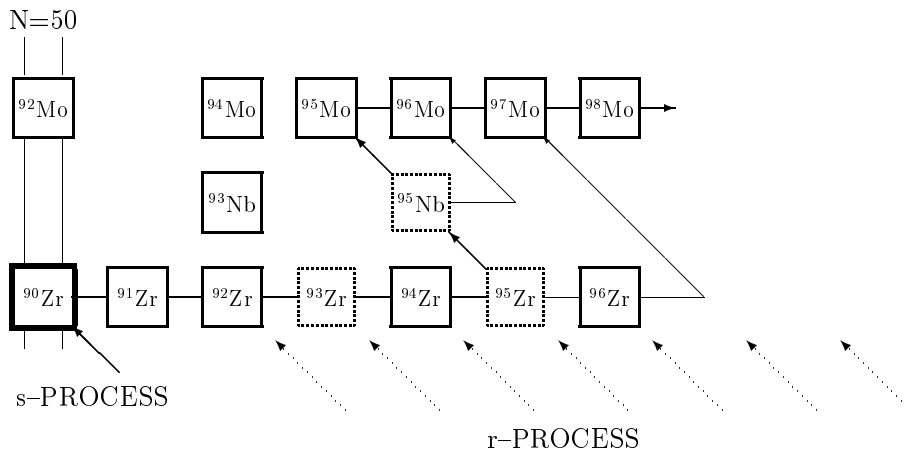


Figure 1: The reaction network around the  $s$ -process branching at  $^{95}\text{Zr}$ . Stable isotopes are indicated by solid boxes. While  $^{93}\text{Zr}$  is practically stable on the time scale of the  $s$  process,  $^{95}\text{Zr}$  acts as a branch point due to the competition between  $\beta$ -decay and neutron capture.  $^{90}\text{Zr}$  is neutron magic and represents a bottle neck for the reaction flow because of its small capture cross section. Possible abundance contributions from the  $r$  process are indicated by dotted arrows.

## 2.2 Neutron magic nuclei

The neutron magic nuclei  $^{90}\text{Zr}$  and  $^{139}\text{La}$  are important because of their small cross sections, which need to be known with good accuracy for a quantitative assessment of the bottle-neck effect on the reaction flow. So far, the remarkable sensitivity of the neighboring abundance pattern to a neutron magic isotope has been demonstrated only in case of  $^{142}\text{Nd}$  [7], where it was possible to confirm the  $s$ -process concept formulated by the stellar model and to reveal the limitations of the classical approach. Accurate data for more of these key isotopes are, therefore, clearly needed.

## 2.3 The $s/r$ -ratio in old stars

The small cross sections of neutron magic nuclei give rise to large  $s$ -process abundances, which dominate the respective  $r$ -process contributions. Therefore, these isotopes can be used for monitoring the  $s$ -process signatures. This argument is particularly important for lanthanum, since this element is completely represented by the neutron magic  $^{139}\text{La}$  ( $^{138}\text{La}/^{139}\text{La} = 10^{-3}$ ). Therefore, lanthanum can be interpreted as an  $s$ -process indicator in stellar spectroscopy, whereas europium represents a typical  $r$ -process element. Comparison of these abundances can be used to characterize the ratio of  $s$ - and  $r$ -process abundances in old, metal poor stars. The  $s$ -process is related to Red Giant stars of 1.5 to 3 solar masses (which evolve slowly) and the  $r$ -process to supernova explosions of massive stars (which evolve quickly). Since the two time scales are so different, the  $s/r$ -ratio is of utmost importance for galactic chemical evolution.

So far barium has been used as an  $s$ -process element because its isotopic cross sections are accurately measured [11]. For technical reasons, lanthanum would be the preferable alternative to use in such studies since it is easier to identify in faint objects. This option requires, however, that the neutron capture cross section be remeasured with sufficient accuracy.

### 3 TECHNOLOGICAL ASPECTS

The neutron cross sections of the Zr isotopes are important for several aspects of traditional and advanced nuclear technologies.

Zirconium is considered the "superstar" among the cladding materials for the production of nuclear fuel elements for all reactor types, including pressurized water reactors (PWRs), boiling water reactors (BWRs), and natural uranium reactors (CANDU). Zirconium alloy materials are the skeletons of fuel assemblies and are used to make the sealed tubes enclosing the fuel pellets. The small neutron capture cross sections in combination with the favorable chemical and mechanical properties are the main advantages for such kind of employments. Obviously, thermal cross sections are of primary importance, but with the present research programs on reactors with fast neutron spectra, including ADS, there is now also a growing demand for the determination of precise capture cross section for fast neutrons. The available information contained in the Nuclear Data libraries is far too uncertain and need to be considerably improved.

In addition to the importance of the cross section for the stable isotopes, the radioactive nucleus  $^{93}\text{Zr}$  ( $t_{1/2} = 1.5 \cdot 10^6$  yr) represents a particular case. In the High Priority Nuclear Data Request List of the Nuclear Energy Agency (NEA/OECD) 5% accuracy are requested for the  $^{93}\text{Zr}(n, \gamma)$  cross section of this long-lived fission product (LLFP) in the entire energy region from thermal to 20 MeV. Since the isotopic enrichment of the available sample material is only 20% and since the cross sections of the stable isotopes could only be determined with uncertainties of typically 10%, the corrections for isotopic impurities prevented to reach this 5% level in the only previous measurement [17]. For this reason, an improved determination of precise cross section data for  $^{93}\text{Zr}(n, \gamma)$  has become a part of the n\_TOF-ADS-ND EC-project.

An additional motivation is that  $^{139}\text{La}$  and the Zr isotopes are very abundant fission fragments. Hence their  $(n, \gamma)$  cross sections have an impact on the neutron balance at high burn-up.

### 4 EXISTING NEUTRON CAPTURE DATA

Quantitative analyses in this field of research have to rely on neutron capture cross section measurements in the energy range from 0.1 to 500 keV. For the proposed isotopes this information is not available for the full energy range and with the necessary accuracy. Even though several measurements exist in parts of the relevant energy range, the results are discrepant by as much as a factor of two, and exhibit unacceptable uncertainties of  $\approx 10\%$  [8], which need to be reduced to  $< 3\%$ .

An illustrative comparison can be made on the basis of Maxwellian averaged stellar cross sections for  $kT=30$  keV, which were derived from the various data sets [8]. In the important case of  $^{90}\text{Zr}$ , values between 11 and 21 mbarn have been reported, for example. Similar discrepancies are found for  $^{92}\text{Zr}$ . These discrepancies are evidence for severe systematic uncertainties due to unrecognized backgrounds, mostly because previous TOF measurements suffered from comparably high sensitivities for scattered neutrons.

Exactly the same situation prevails for  $^{139}\text{La}$ . Existing data differ by factors of two and suffer from the very same problems as discussed for the Zr isotopes [8].

More precise data are available for  $^{94}\text{Zr}$  and  $^{96}\text{Zr}$ , but only for a particular stellar temperature corresponding to a thermal energy of 25 keV. These measurements were carried out via activation in the quasi-stellar spectrum obtained by means of the  $^7\text{Li}(p, n)^7\text{Be}$  reaction [12, 13]. According to the most advanced stellar *s*-process models, this temperature is reached during the helium shell flashes in AGB stars, which account for only

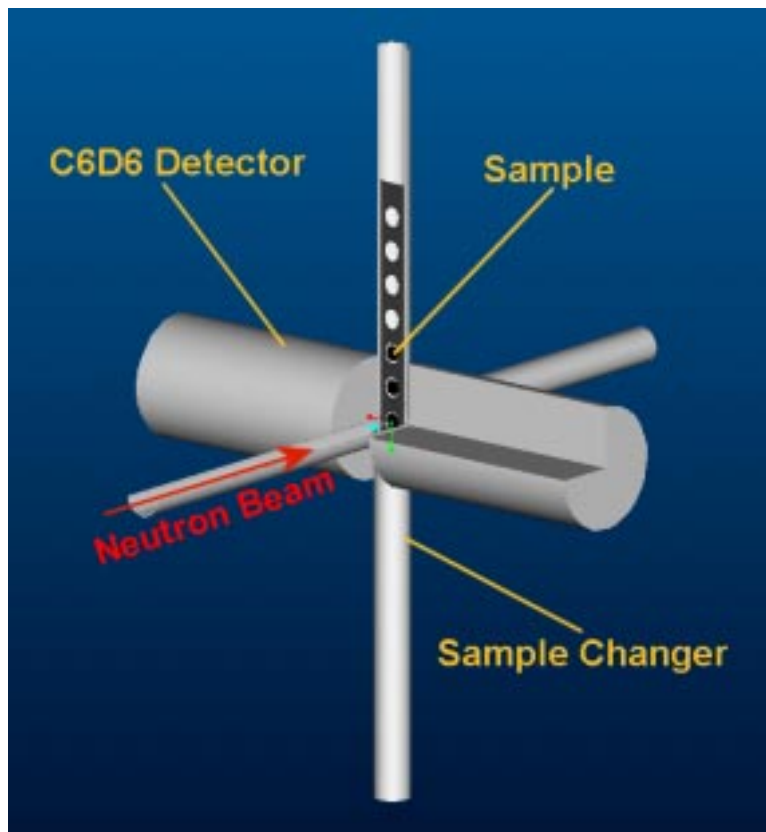


Figure 2: Schematic drawing of the detectors to be used as arranged around the beamline. The beam direction is indicated by the red arrow. One of the detectors and part of the sample changer are cut away in order to show the sample changer strip and the samples.

$\approx 5\%$  of the  $s$ -process neutron exposure. The remaining 95%, however, are processed at a considerably lower temperature of  $kT=8$  keV [14, 15]. One of the difficulties with previous measurements is that data are reported only for neutron energies above approximately 3 keV. In an environment with energy distributions peaked at 8 keV, it is important to cover the neutron energy range down to 0.1 keV, especially for isotopes with strong, low energy resonances. Since all Zr isotopes, and  $^{90}\text{Zr}$  in particular, fall into this category, new measurements with improved accuracy and complete coverage of the relevant neutron energy range are urgently required. The CERN n\_TOF facility puts precisely this problem within reach.

## 5 PROPOSED MEASUREMENTS AT n\_TOF

In order to address the needs for improved data, we propose to measure the  $(n,\gamma)$  cross sections of  $^{90-94}\text{Zr}$ ,  $^{96}\text{Zr}$ , and  $^{139}\text{La}$  at the n\_TOF facility. These cross sections will be determined from 1 eV to 500 keV using two  $\text{C}_6\text{D}_6$  liquid scintillator detectors, which are optimized for minimal neutron sensitivity by replacing the traditional aluminum housing for the liquid scintillator by a thin carbon fiber shell [16]. In this way, crucial and previously neglected or underestimated backgrounds due to sample scattered neutrons can be significantly reduced, thus enhancing the ability to determine weak resonances. The samples will be mounted in the standard carbon fiber sample changer. Capture  $\gamma$ -rays will be registered by means of two  $\text{C}_6\text{D}_6$  scintillator detectors arranged as pictured in Fig. 2.

Highly enriched samples of the stable isotopes will be borrowed from Oak Ridge

National Laboratory (ORNL) and/or from IPPE Obninsk.  $^{139}\text{La}$  is commercially available. The  $^{93}\text{Zr}$  sample, which consists of purified fission zirconium will be loaned either from Oak Ridge or, preferentially, from Petten. Because of the comparably low  $^{93}\text{Zr}$  content of 20%, it is important to determine the isotopic corrections from the cross section results obtained in the same experiment with the Zr stable isotopes. Compared to a first attempt, where the measurement was hampered by a strong background of 5kHz from the radioactivity of the sample [17], the n\_TOF experiment on  $^{93}\text{Zr}$  will be far superior thanks to the 1000 times better duty cycle.

The measurements are expected to yield cross section uncertainties of typically 3% for the stable isotopes, about three times smaller than reported in previous work [8]. Estimates for the unstable  $^{93}\text{Zr}$  sample yield a somewhat larger uncertainty of about 5% because of the low enrichment. The accuracy aimed at with respect to the nucleosynthesis problems will also satisfy the request from the ADS application.

The respective sizes and enrichments are listed in Table 1.

Isotope	Mass (g)	Enrichment (%)	Supplier	Protons Needed
$^{90}\text{Zr}$	2	97.7	Obninsk	$3 \times 10^{17}$
$^{91}\text{Zr}$	1	89.9	Obninsk	$2 \times 10^{17}$
$^{92}\text{Zr}$	1	91.7	Obninsk	$3 \times 10^{17}$
$^{93}\text{Zr}$	6.6	20	Petten	$3 \times 10^{17}$
$^{94}\text{Zr}$	1.5	91.8	Obninsk	$3 \times 10^{17}$
$^{96}\text{Zr}$	4	58.5	Obninsk	$3 \times 10^{17}$
	3	95.6	ORNL	$3 \times 10^{17}$
$^{139}\text{La}$	2	100	commercial	$2 \times 10^{17}$

Table 1: The samples for the measurements proposed at the CERN n\_TOF facility. Also listed are the requested number of protons.

Based on the experience with the successful capture experiments performed so far (TOF03, TOF04, and TOF05) we estimate that one week of beam time will be needed for each of the isotopes. These estimates assume that n\_TOF is operating in dedicated mode. If more than one pulse is available per PS supercycle, or if the experiment were run in parasitic mode, then these times would change correspondingly. Fig. 3 illustrates the expected count rates per bunch of  $7 \times 10^{12}$  protons and for a resolution of 500 bins per decade corresponding to a resolution in neutron energy of  $\simeq 1\%$  (Zr and  $^{139}\text{La}$  samples, respectively). In all cases, the signal/background ratio is expected large enough to allow safe cross section analyses.

## 6 ASTROPHYSICAL IMPLICATIONS

Once the stellar cross sections of the investigated isotopes have been deduced from the differential TOF data, the corresponding reaction rates will be incorporated into the FRANEC code for modeling the He burning zones in Red Giants [18] for a quantitative investigation of the *s*-process features described in Sec. 2. This part of the proposed study will be performed in collaboration with R. Gallino and his co-workers, and will include a detailed account of the astrophysical quests related to abundance observations in Red Giants and presolar grains as well as the galactic chemical evolution aspects connected with observed *s/r*-ratios.



## References

- [1] E. Burbidge, G. Burbidge, W. Fowler, and F. Hoyle, *Rev. Mod. Phys.* **29**, 547 (1957).
- [2] P. Seeger, W. Fowler, and D. Clayton, *Ap. J. Suppl.* **97**, 121 (1965).
- [3] F. Käppeler *et al.*, *Ap. J.* **257**, 821 (1982).
- [4] D. Lambert *et al.*, *Ap. J.* **450**, 302 (1995).
- [5] A. Davis *et al.*, in *Nuclei in the Cosmos V*, edited by N. Prantzos and S. Harissopulos (Editions Frontières, Paris, 1998), pp. 563 .
- [6] M. Lugaro *et al.*, *Ap.J.*, submitted .
- [7] C. Arlandini *et al.*, *Ap. J.* **525**, 886 (1999).
- [8] Z. Bao *et al.*, *Atomic Data Nucl. Data Tables* **76**, 70 (2000).
- [9] F. Käppeler, *Prog. Nucl. Part. Phys.* **43**, 419 (1999).
- [10] K. Toukan and F. Käppeler, *Ap. J.* **348**, 357 (1990).
- [11] F. Voss *et al.*, *Phys. Rev. C* **50**, 2582 (1994).
- [12] H. Beer and F. Käppeler, *Phys. Rev. C* **21**, 534 (1980).
- [13] K. Toukan, K. Debus, F. Käppeler, and G. Reffo, *Phys. Rev. C* **51**, 1540 (1995).
- [14] O. Straniero *et al.*, *Ap. J.* **440**, L85 (1995).
- [15] M. Busso, R. Gallino, and G. Wasserburg, *Ann. Rev. Astron. Astrophys.* **37**, 239 (1999).
- [16] R. Plag *et al.*, in *Interaction of Neutrons with Nuclei*, edited by W. Furman (JINR, Dubna, 2000), pp. 181 ;  
Nucl. Instr. Meth. A, in press .
- [17] R. Macklin, *Astrophys. Space Sci.* **115**, 71 (1985).
- [18] A. Chieffi and O. Straniero, *Ap. J. Suppl.* **71**, 47 (1989).

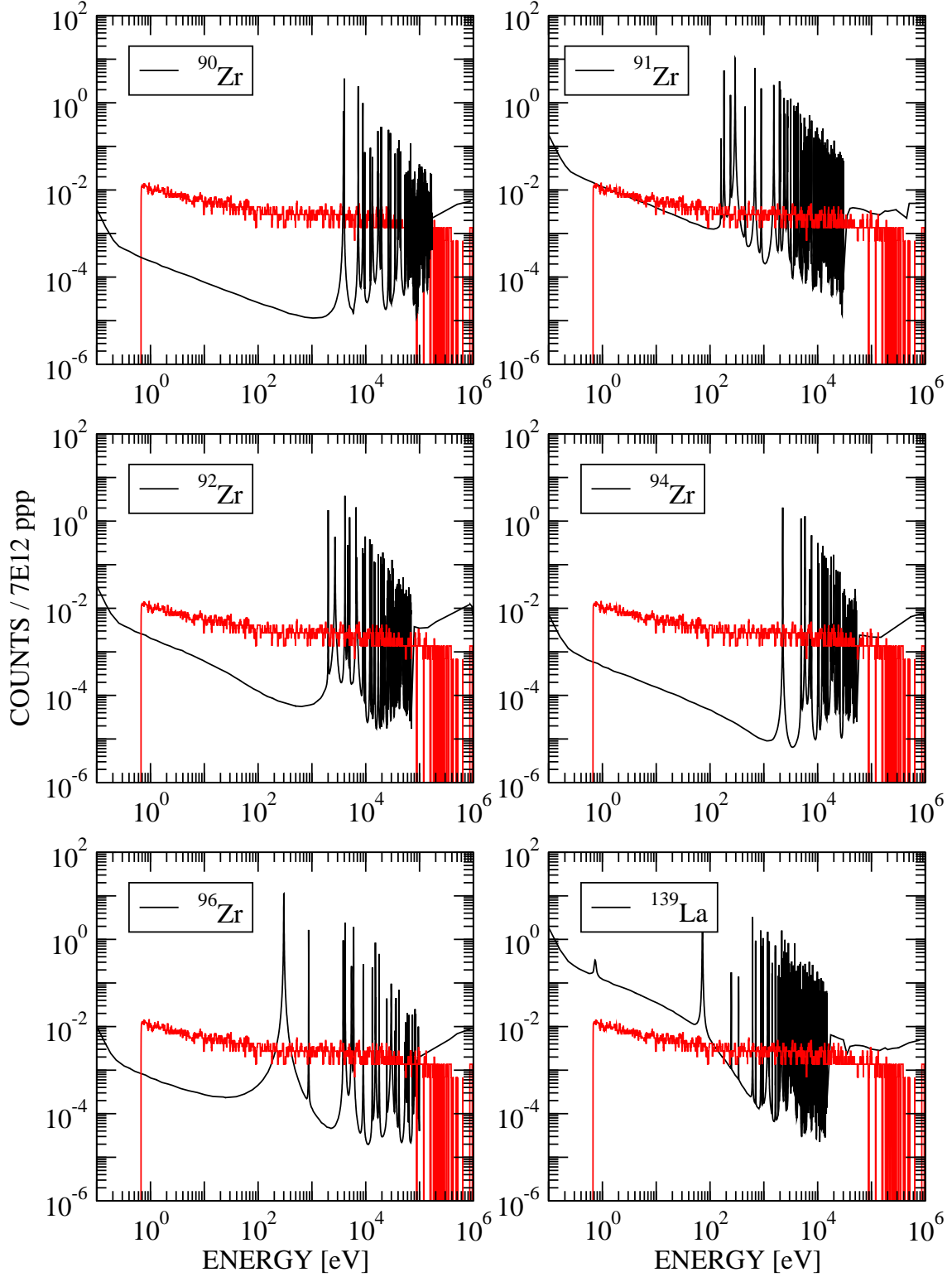


Figure 3: The estimated count rates for the proposed experiments (stable targets). The abscissa is neutron energy while the ordinate is the estimated number of events per nominal proton bunch of  $7 \times 10^{12}$  protons. The count rates are based on the sample masses listed in Table 1, and the detection efficiency for capture events is assumed as 10%. The energy grid of 500 bins per decade corresponds to a resolution in neutron energy of  $\Delta E/E \simeq 1\%$ . The expected background (red histogram) has been determined by proper adjustment of the experimental spectra measured so far.